NASA Investigation of Flow Direction Effects on Impedance Eduction for Acoustic Liners

M. G. Jones*, D. M. Nark†, and B. M. Howerton‡
NASA Langley Research Center, Hampton, VA 23681-2199, U.S.A

In support of a collaboration with the International Forum for Aviation Research (IFAR), the NASA Langley Liner Physics Team has acquired a detailed dataset for use in the evaluation of flow direction effects on the acoustic liner impedance eduction process. Measurements are acquired with four acoustic liners designed to cover a range of sensitivities to source sound pressure level and tangential mean flow effects, specifically at source levels of 120 and 140 dB and centerline Mach numbers of 0.0, 0.1, 0.2, and 0.3. These measurements include detailed flow profile surveys upstream and downstream of the liner test window, as well as acoustic pressure data over the extent of the test window. The results clearly demonstrate the importance of the choice of Mach number used in the impedance eduction analysis. Average Mach number differences of less than 0.01 result in significant variation in the educed impedance spectra. These data will soon be supplied to the IFAR partners and will be made available for the general public within the next year.

I. Introduction

This paper is intended to provide details regarding NASA results for *Challenge 5* of the acoustic liner topic conducted in support of the International Forum for Aviation Research (IFAR). The IFAR consists of representatives from a number of national research laboratories and was established to enable information exchange on fundamental aviation research activities. Three challenges[1] were initiated in 2017 for comparisons of (1) manufacturing, data acquisition, and impedance eduction approaches, (2) 3-D aeroacoustic propagation codes for evaluation of spanwise variable impedance liners, and (3) approaches to efficiently evaluate multizone acoustic liners. Two additional challenges were initiated in early 2021. *Challenge 4* explores the effects of sound source type and level on the acoustic impedance of a liner. The initial NASA contribution to this challenge is provided in a companion paper.[2]

The focus of the current paper is *Challenge 5,* which targets an improved understanding of the effects of flow direction on the acoustic impedance educed for a liner mounted in a grazing flow duct. This topic has been of great interest to the acoustic liner community for the last decade.[3–8] Most researchers tend to fall into one of two schools of thought. The first group assumes the acoustic impedance of the liner to be independent of the flow direction, although it is affected by other changes in the aeroacoustic environment that often accompany a change in flow direction. The second view is that the liner has a distinct acoustic impedance depending on the flow direction. It is the view of the authors that the correct answer (i.e., how one defines impedance) may lie somewhere between the two. Nevertheless, it is the purpose of this challenge to gain clarity on this issue.

In support of this challenge, the NASA Liner Physics Team has acquired a detailed dataset suitable for more rigorous evaluation of the effects of flow direction on the impedance educed with conventional acoustic liners. Four acoustic liners with different levels of nonlinearity are included in this study. These liners are tested in the NASA Langley Grazing Flow Impedance Tube (GFIT, see Fig. 1) at two source sound pressure levels (SPLs of 120 and 140 dB), four flow conditions (centerline Mach numbers of 0.0, 0.1, 0.2,

*Senior Research Scientist, Research Directorate, Applied Acoustics Branch, AIAA Associate Fellow.
†Senior Research Scientist, Research Directorate, Applied Acoustics Branch, AIAA Associate Fellow.
‡Research Scientist, Research Directorate, Applied Acoustics Branch, AIAA Senior Member.

and 0.3), and with the source sequentially placed upstream and downstream of the test window. Detailed flow profiles acquired across axial planes located just upstream and downstream of the liner test window are used to estimate the 2-D flow profiles that are present over the acoustic liner. Acoustic data are acquired via microphones flush-mounted in the rigid walls throughout the test window. A portion of these are used in the current study to educe the surface impedance of the liner. This full dataset (flow and acoustic data) will be provided to each IFAR participant (and later, to the general public), such that they can process the data using their respective tools and assumptions.

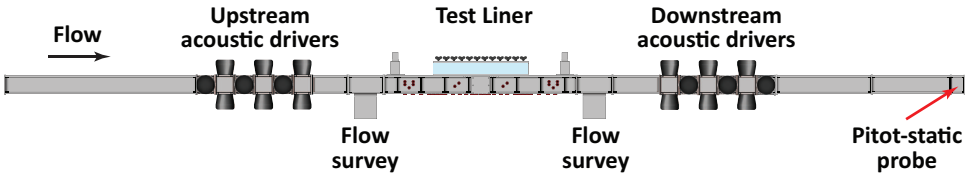

Figure 1: **Sketch of the NASA Grazing Flow Impedance Tube (GFIT).**

The remainder of this paper is organized as follows. Section II provides a description of the flow duct (GFIT), four test liners, and measurement approaches used to acquire mean flow and acoustic data. Section III presents the analyses used by NASA for evaluation of flow and acoustic data. Results are presented in Section IV, and key findings are summarized in Section V.

II. Experimental Setup

Details are presented in this section regarding the flow duct and the measurement apparatuses used to determine the mean flow and acoustic field properties.

A. Grazing Flow Impedance Tube

The GFIT is typically used to measure the acoustic characteristics of liners placed in the walls of subsonic aircraft engine nacelles. This 2.0"×2.5" waveguide (Figs. 1 and 2) contains upstream and downstream source sections each consisting of 12 acoustic drivers. Flow survey systems are located immediately upstream and downstream of the test window, such that changes in flow profile over the length of the liner can be assessed. Static pressure ports are also distributed along the lower wall of the duct. The surface of the test liner forms a portion of the upper flow surface of the GFIT, and 95 microphones are flush-mounted in the walls of the test window. Near-anechoic terminating diffusers are included at each end of the duct to control reflections and reduce overall flow noise. Finally, interchangeable blank sections are included to allow reconfiguration of the duct.

To generate the desired flow conditions, pressurized and heated air is supplied to the inlet of the GFIT, while a vacuum system is employed at the duct exit to evacuate air from the tube. With this arrangement, static pressure at the test section can be held to near-ambient conditions at all flow velocities with constant total temperature. A pitot-static probe mounted near the downstream termination of the GFIT is used to set the desired centerline Mach number (labeled setpoint Mach number, M_{SP}), ranging from Mach 0.0 to 0.3 in the current study.

B. Test Liners

Four liners are chosen to cover a variety of impedance spectra over the frequency range of interest. The first liner, labeled CSQ3, is a 16.0"-long liner containing a 19×304 array of 0.05"×0.05"×3.0" chambers. Due to the small cross section of each chamber, no facesheet is needed to provide suffient resistance. With a chamber length-to-diameter ratio of 60, this liner is expected to be insensitive to changes in source SPL and grazing flow velocity.[9] The CSQ3 liner is additively manufactured from a polymer resin using a stereolithography (SLA) process and is of particular interest because its surface impedance can be accurately predicted from first principles.[10]

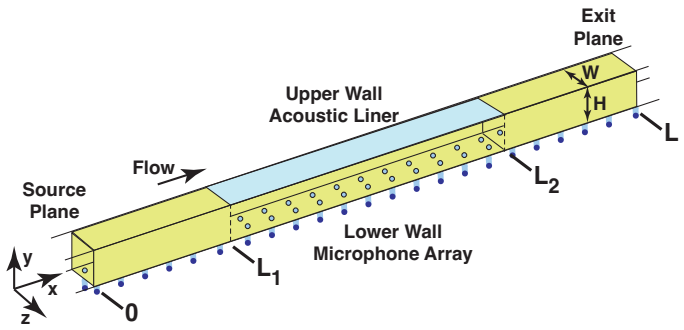

Figure 2: **Sketch of the Grazing Flow Impedance Tube test window.**

The second liner, labeled C1R27, has a length of 23.5". It consists of a 270 MKS Rayls wire mesh mounted over a 1.5"-deep core. This core is filled with hexagonal aluminum honeycomb, with flat-to-flat spacing of 0.375". This configuration is chosen because it also has limited sensitivity to changes in SPL and Mach number, and the surface impedance, ζ, can be predicted as

$$\zeta = \frac{R_f}{\rho c} - i \cot(kh), \tag{1}$$

where R_f is the wire mesh DC flow resistance, ρ and c are the density and sound speed of ambient air, respectively, k is the freespace wavenumber, and h is the chamber height. A sign convention of $\exp[i\omega t]$ is assumed, where ω and t are the angular frequency and time, respectively.

The last two liners, IU2 and IU2T, are 15.5"-long liners additively manufactured using SLA resin. Each of these liners consists of a 4×30 array of 0.4"×0.4"×2.0" chambers and contain nearly identical integrated facesheets. There are 22 perforations with a diameter of 0.041" positioned over each chamber such that they do not interface with the 0.13"-thick solid partitions that separate the chambers. This results in a chamber active surface open area ratio of 0.18. The thickness of the facesheet for the IU2 liner is 0.034", which is a fairly standard thickness for conventional engine nacelle liners. With a hole thickness-to-diameter ratio of 0.8, this liner is designed to be weakly nonlinear, i.e., to exhibit minimal sensitivity to differences in source SPL and grazing flow velocity. The thickness of the facesheet for the IU2T liner is 0.25". With a hole thickness-to-diameter ratio of 6.1, this liner should be more linear than the IU2 liner. Nevertheless, given the high open area ratio, both of these (IU2 and IU2T) liners are expected to be linear.

Data acquired with each of these liners are included in the package to be made available later this year. However, the results in the current paper are limited to the CSQ3 and IU2 liners as these are sufficient to demonstrate the key points. Results for the C1R27 and IU2T liners exhibit very similar features.

C. Flow Surveys

Each flow survey section contains a dual-axis traverse system used to position a total pressure pitot probe at any location within the axial plane. Two pitot probes are successively used for this measurement (see Fig. 3). The first is shaped to allow detailed measurements close to the upper wall and covers the range of $\{1.000" \leq y \leq 2.482", 0.125" \leq z \leq 1.875"\}$. Similarly, the second is shaped to enable measurements near the lower wall and covers the range of $\{0.018" \leq y \leq 1.500", 0.125" \leq z \leq 1.875"\}$. Vertical limits near the upper and lower walls are determined by the diameter of the flattened tips of the pitot probes and lateral limits are set by the half-diameter of the probe support tube. Measurement points are clustered near the upper and lower walls to increase the resolution in those areas. A port located on the centerline of the lower wall of each traverse section, in-plane with the probe tip, is used to measure local static pressure. As shown in Figure 1, these measurements are performed immediately fore and aft of the test window that would typically contain the test liner. However, a hardwall insert is installed for these surveys.

For efficiency, pitot probes are mounted in both the upstream and downstream windows simultaneously, such that data can be sequentially acquired at both locations while the mean flow is maintained. To avoid

interference effects, the inactive probe is positioned against the wall on the opposite side of the duct from the active probe and is fully retracted.

As noted earlier, the desired centerline Mach number is set at the location of the pitot-static probe near the duct termination. Each dual-axis traverse probe system is used to measure the total pressure profile at 29 vertical locations between the lower and upper walls at 9 spanwise locations within the duct. Each probe is used to measure more than half of this array, such that the overlap data can be used to ensure reliability of the total dataset. These total pressure profiles are combined with static pressure measurements in the same axial planes to compute Mach numbers at each measurement location (assuming isentropic flow). When combined with the known velocities (zero) at the walls, this provides a full 2-D shear flow profile at both axial planes.

The acoustic analysis (Sec. III.B) assumes an average Mach number is known at the axial midpoint of the acoustic liner. This value is computed as a prorated average of the upstream and downstream measurements, i.e., the Mach number is assumed to linearly vary between the two flow survey axial planes. This approximation is expected to be within the margin of uncertainty given the proximity of the two measurement planes to the axial midpoint of the liner.

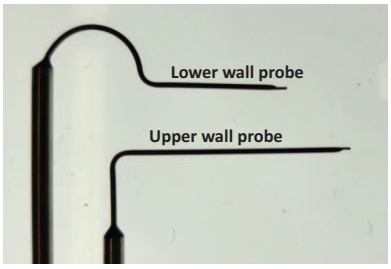

Figure 3: **Pitot probes used to measure flow profile in the Grazing Flow Impedance Tube.**

Static pressure ports are mounted in the GFIT lower wall over the axial extent of $\{-150" \leq x \leq 127"\}$, where $x = 0"$ represents the axial plane at the upstream end of the computational domain and the leading edge of the acoustic liner is at $x = 8"$. Note that these pressures could be used to get an estimate of the relative drag generated by each liner. However, due to the very small changes in static pressure over the length of the liner, higher precision measurement instrumentation is needed to properly assess this drag.

D. Acoustic Surveys

For the current test, sound pressure levels of 120 and 140 dB are considered. This level is set as the peak level within $\pm 1.0"$ of the edge of the liner closest to the source that is currently engaged (i.e., the leading or trailing edges of the liner). Acoustic data are then simultaneously acquired with the 95 microphones using a swept sine excitation[11] to cover the frequency range of 400 to 3000 Hz. The acoustic pressures measured at all 95 microphone locations will be provided to the IFAR partners for more detailed evaluation. Twelve microphones positioned on the lower wall opposite the liner are used by NASA to educe the liner impedance via the Prony method.[12]

III. Analysis

This section provides a description of the method used to compute the 2-D flow profiles based on the measured dataset. It also provides a brief summary of the Prony method for impedance eduction.

A. Flow Computations

The full 2-D profiles upstream and downstream of the liner are obtained via fits to the Mach numbers determined across the 11×31 array (includes Mach 0.0 at the rigid walls) of measurement locations. The two readings (one by each probe) in the overlap region ($1.0" \leq y \leq 1.0"$) are averaged, and the remaining data are normalized to match Mach number values at $y = 1.0"$ and $1.5"$. The resultant Mach number distribution

at each axial plane is then fit to a Non-Uniform Rational B-Spline (NURBS) surface. The Mach number values are integrated over this surface to obtain the average Mach number.

These 2-D profiles are used to compute boundary layer thickness, δ, displacement thickness, δ^*, and momentum thickness, θ, respectively, at the upper and lower walls. Corresponding values are also computed using the 1-D spanwise-centered data ($0.0" \leq y \leq 2.5", z = 1.0"$).

B. Acoustic Computations

The Prony Method[12–14] is used with the acoustic pressures acquired along the wall opposite the liner to educe the acoustic impedance of the test liner. This analysis assumes the liner has infinite length and the sound field is unidirectional. Since our liners have finite length, it is therefore important to constrain our application of this method to that portion of the sound field where the sound field remains predominately unidirectional. To approach this condition, microphones positioned opposite the liner but away from the leading and trailing edges of the liner are used. The first and last microphones are positioned such that the effects of reflections from the leading and trailing edges of the liner are minimal. Application of this method for liner impedance eduction has been described in earlier papers. The axial wavenumber is determined from the acoustic pressures measured with the microphones on the wall opposite the uniform-impedance liner. This wavenumber is input to the Myers impedance boundary condition[15] to compute the impedance of the test liner. The impedances computed in this manner are then run through a mean filter to smooth the spectrum, as the true impedance spectrum is assumed to be a smooth function of frequency.

IV. Results

A. Flow Surveys

Figure 4 provides 1D flow profiles acquired upstream and downstream of the test window along the spanwise centerline of the duct ($z = 1.0"$). Figure 5 presents the corresponding 2D flow profiles. Although the changes are not large, the downstream profiles exhibit a clear flattening (slightly larger core) relative to the upstream profiles. Recall that the setpoint Mach number is set at an axial location well downstream of the test window. As a result, the centerline Mach numbers measured upstream and downstream of the test window diverge from the setpoint Mach number as the flow rate is increased.

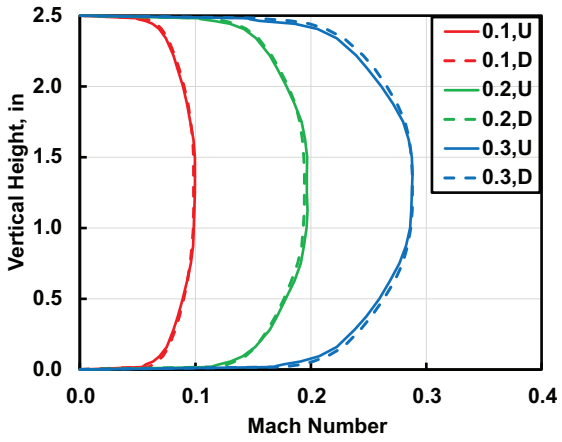

Figure 4: **1D flow profiles, $M_{1D}(y, z = 1.0")$, measured upstream (U) and downstream (D) of the test window for setpoint Mach numbers of 0.1, 0.2, and 0.3.**

Figure 6 provides a comparison of flow parameters derived from these 2D and 1D flow profiles. Previous studies[7,16] have demonstrated that the educed impedance is very sensitive to the choice of Mach number

used in the eduction analysis. Therefore, it is of interest to explore the difference in impedances educed using each of these two average Mach numbers. Average Mach numbers (Fig. 6a) show linear trends, given by

$$\begin{matrix} M_{\mathrm{1D,ave}}(z = 1.0") = 0.87 M_{\mathrm{SP}} \\ M_{\mathrm{2D,ave}} = 0.78 M_{\mathrm{SP}} \end{matrix} . \tag{2}$$

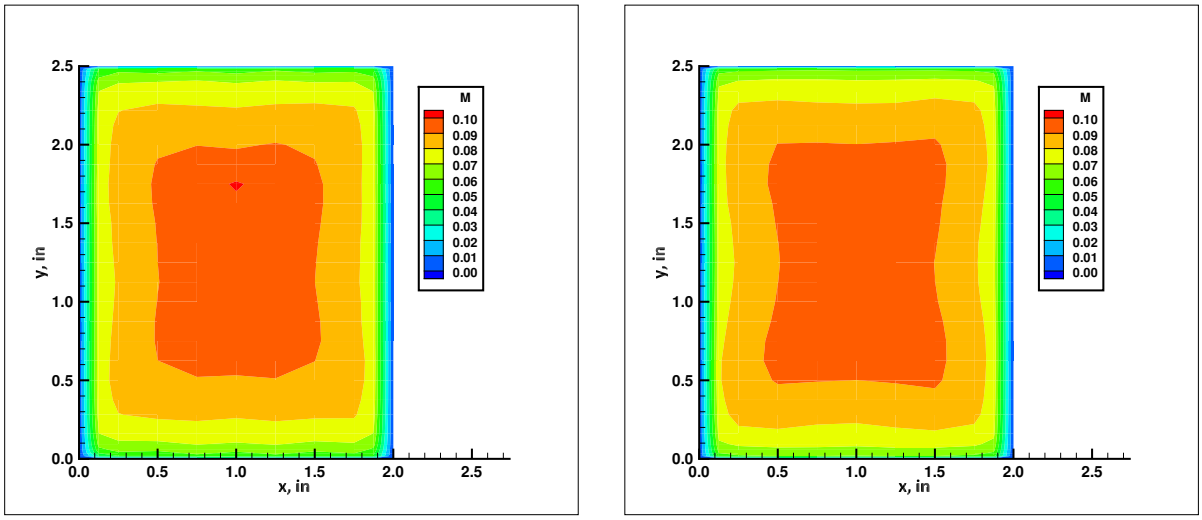

(a) $M_{\mathrm{SP}} = 0.1$, **upstream.**

(b) $M_{\mathrm{SP}} = 0.1$, **downstream.**

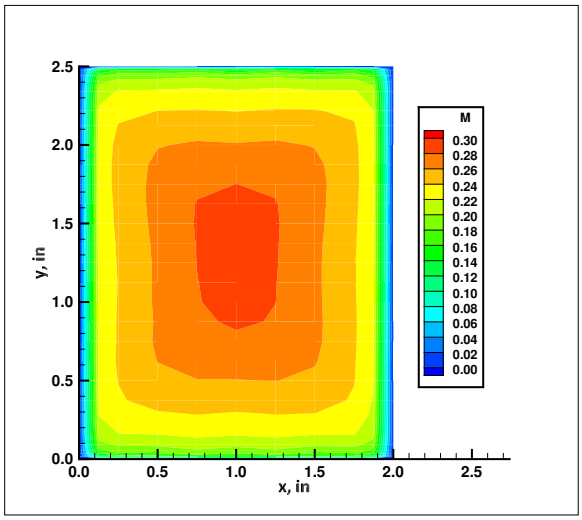

(c) $M_{\mathrm{SP}} = 0.3$, **upstream.**

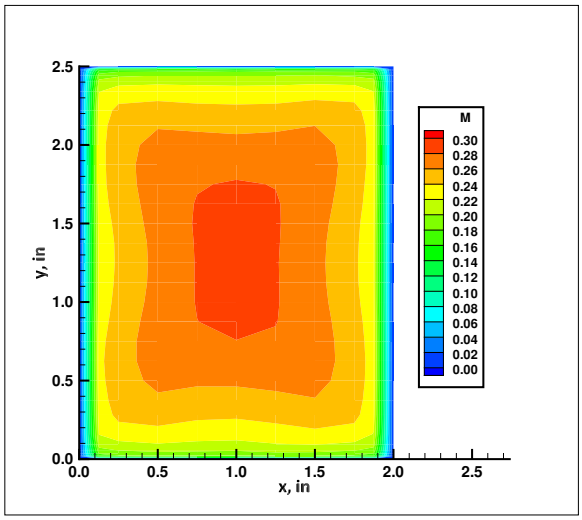

(d) $M_{\mathrm{SP}} = 0.3$, **downstream.**

Figure 5: **Comparison of upstream and downstream 2D flow profiles, M_{2D}. Note the change in color scales for the two flow conditions.**

The corresponding boundary layer parameters for the lower and upper walls of the flow duct are presented in parts 'b - d' of Figure 6. A prorated average, based on the location of the axial midpoint of the liner, of the upstream and downstream results is used for analysis of the acoustic liners. This assumes the average Mach number to vary linearly between the two measurement locations. In reality, the Mach number variation is not truly linear. However, it is not expected to deviate much from the linear assumption over this small axial distance. The 1D boundary layer thicknesses are observed to hover near 0.9" over this range of flow conditions, with the lower wall readings slightly higher than those measured for the upper wall. The corresponding 2D boundary layer thicknesses are lower, with an average value near 0.7". However, there is more separation between the lower and upper wall results for the 2D dataset as compared to the 1D data.

The corresponding 1D and 2D displacement thicknesses are approximately 0.125" and 0.080", respectively, while the corresponding 1D and 2D momentum thicknesses are approximately 0.095" and 0.060".

Figure 7 provides static pressure axial profiles measured over the portion of the GFIT that corresponds to the computational domain used in the acoustic analysis. Results are provided for setpoint Mach numbers of 0.1, 0.2, and 0.3, with the IU2 liner installed. These static pressures are provided relative to the atmospheric pressure, P_a, that was present at the time of the test. The relative static pressure ($P_s - P_a$) is set to zero at the axial midpoint ($x = 20$") of the liner window, i.e., the location where a liner can be mounted. The slopes of these profiles appear to be linear over this axial extent. However, these curves become slightly steeper near the leading edge of the liner.

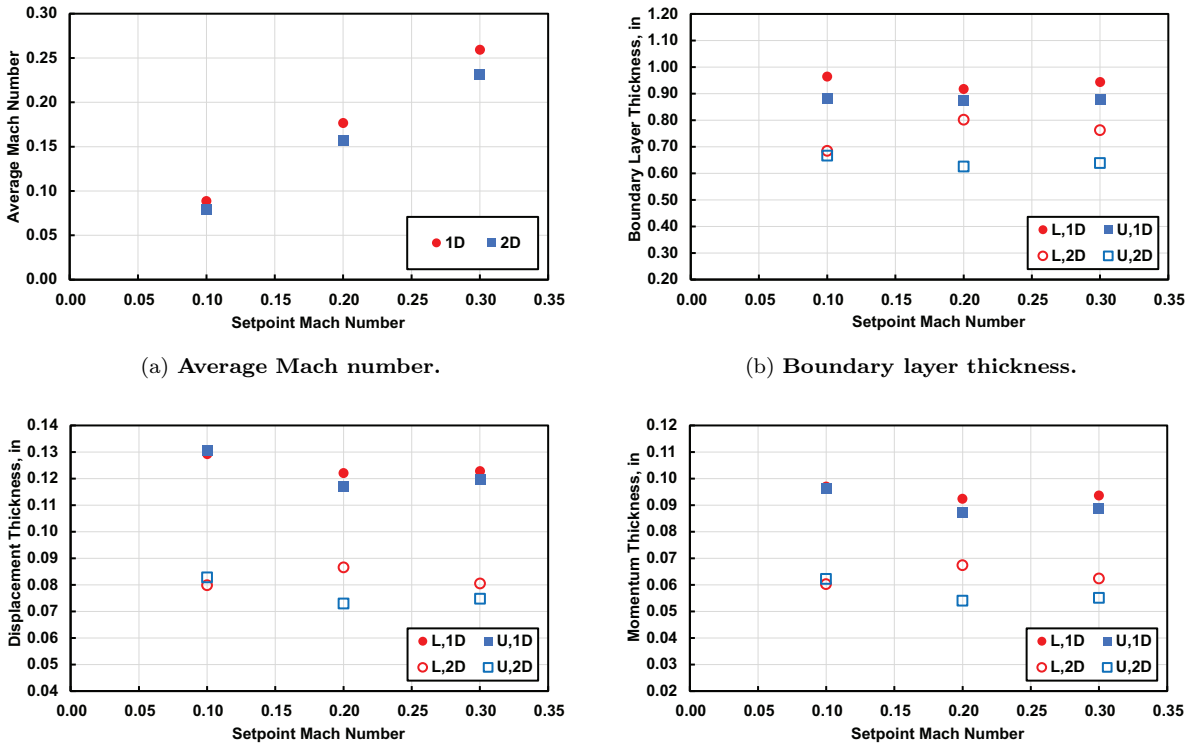

(a) **Average Mach number.**

(b) **Boundary layer thickness.**

(c) **Displacement thickness.**

(d) **Momentum thickness.**

Figure 6: **Lower (L) and upper (U) wall boundary layer parameters based on 1D and 2D flow profiles.**

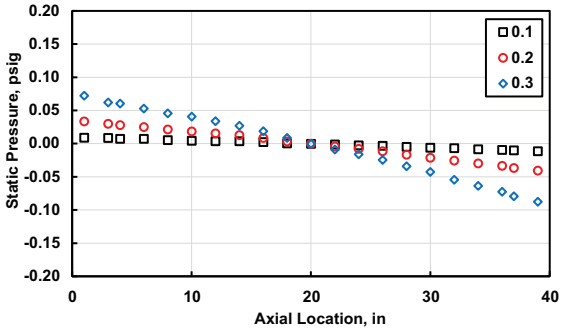

Figure 7: **Axial static pressure profiles for setpoint Mach numbers of 0.1, 0.2, and 0.3; IU2 liner.**

B. Acoustic Surveys

Figure 8 presents axial SPL profiles acquired at three arbitrarily selected frequencies (1.0, 1.5, and 2.0 kHz) with the CSQ3 and IU2 liners sequentially installed in the GFIT. The setpoint Mach number is 0.3 for each of these datasets. The location of the liner is depicted via the hashed box at the bottom of the figure. Solid and dashed lines are used to represent the data acquired with the source upstream and downstream of the liner, respectively. For these tests, the source level was set to 140 dB near the liner edge closest to the source. The effects of flow direction are clearly noticeable for both datasets.

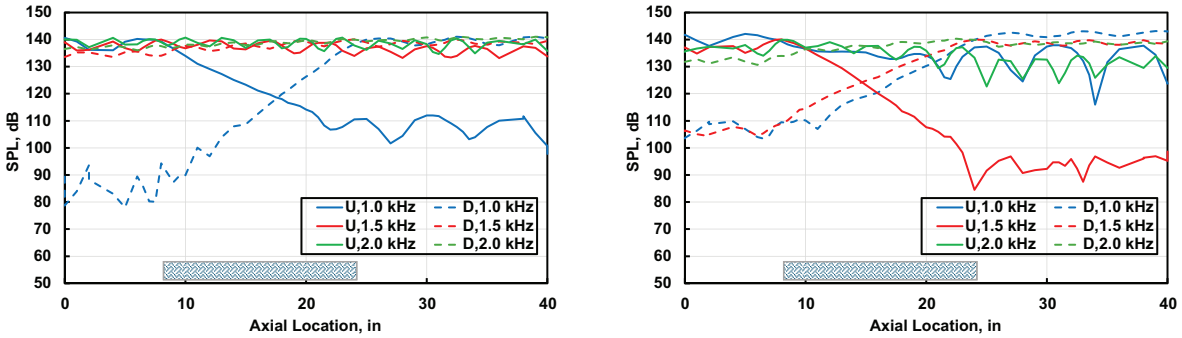

(a) **CSQ3 liner.** (b) **IU2 liner.**

Figure 8: **Axial SPL profiles for upstream (U) and downstream (D) sources; location of liner is denoted via hashed box;** $M_{\mathrm{SP}} = 0.3$**.**

Observe that the attenuation for the CSQ3 liner is negligible at 2.0 kHz, and increases slightly at 1.5 kHz. However, there is significant attenuation at 1.0 kHz, slightly greater than 30 dB for the upstream source and approximately 50 dB for the downstream source. For the downstream source, the results become somewhat disjoint at the upstream end (near $x = 0.0$"). In contrast, note that the SPLs for the upstream source are sufficient to achieve a higher signal-to-noise ratio, thereby resulting in a smoother profile. Recall that the source used in this study is a swept sine. The ability to extract a clean signal with decreasing signal-to-noise ratio is dependent on the time duration used for the sine sweep. Therefore, these results suggest that a longer sweep time may be needed. Another option would be to change the source type to stepped sine (one frequency at a time), but this would greatly increase the data acquisition time. Nevertheless, the data over the length of the liner are sufficiently smooth to enable application of the Prony method to educe the liner impedance. The corresponding SPL profiles for the IU2 liner are provided in Figure 8b. Note that there is about 50 dB attenuation at 1.5 kHz with the upstream source, while about 30 dB attenuation is achieved at both 1.0 and 1.5 kHz with the downstream source.

These results confirm that there are clear differences between the attenuation rates for upstream and downstream propagation. Restated, the optimum impedance spectra are different for downstream and upstream propagation. Regardless, since these liners are quite linear, the impact of this varied attenuation will have limited effect on the educed impedance. However, the educed impedance for nonlinear liners (e.g., perforate-over-honeycomb liners with low open area ratios) is very sensitive to changes in the SPL. For this type of liner, a sensitivity to SPL will be manifested as a sensitivity to flow direction simply due to the resultant change in SPL at the liner surface.

The four liners included in the current study were initially chosen to cover a range of linearity. Indeed, the IU2 perforate-over-honeycomb liner is more nonlinear than the others used in this study. However, the range of SPL used in this study (120 dB to 140 dB) is insufficient to evaluate this nonlinearity. Specifically, the results achieved with each of the test liners are very similar for source SPLs of 120 dB and 140 dB. Thus, for convenience, only the results for the 140 dB case are included in this paper.

Figure 9 presents the impedance spectra educed for the CSQ3 liner with a source SPL of 140 dB, using both upstream and downstream sources. Figure 9a provides results achieved for a no-flow condition. As expected, the two impedance spectra are observed to be nearly identical. Parts 'b' and 'c' of this figure provide the corresponding educed impedance spectra for data acquired at a setpoint Mach number of 0.3. For Figure 9b, the 1D average Mach number (0.259) is used with the Prony method for the eduction process. The large resistance peak near antiresonance is perhaps the most informative component of the impedance spectra. Note that the peak frequency moves from around 2.0 kHz for the upstream source to about 2.5 kHz for the downstream source. For comparison, Figure 9c presents the educed impedance spectra for which the 2D average Mach number (0.231) is used in the analysis. For this choice, the ordering is switched such that the peak frequency for the upstream source is about 2.2 kHz while that for the downstream source is near 2.0 kHz. ***Clearly, the choice of Mach number used in the analysis is critical to the accurate determination of the impedance.*** Finally, Figure 9d provides a comparison of impedance spectra educed at setpoint Mach numbers of 0.1, 0.2 and 0.3. For these eductions, an upstream source was employed and the Prony method analysis was conducted using 2D average Mach numbers of 0.079, 0.157, and 0.231. A slight increase in the frequency of maximum resistance is observed as the Mach number is increased. Nevertheless, this frequency shift over the full range of Mach numbers is on the order of 100 Hz, much less than the differences observed between impedances educed using the 1D and 2D averaged Mach numbers.

Corresponding results for the IU2 liner are presented in Figure 10. Other than some anomalous behavior at the very low frequencies (due to transients at startup of the frequency sweep), the impedances educed in the absence of mean flow are independent of the source location. Similar to the CSQ3 results, the shapes of the impedance spectra change with choice of Mach number (i.e., 1D or 2D). The frequency of peak resistance (just below antiresonance in this case) is higher for the upstream source when using the 1D average Mach number, but is higher for the downstream source when using the 2D average Mach number. Again, these effects of the Mach number chosen for use in the analysis are much larger than those observed for data acquired at setpoint Mach numbers of 0.1, 0.2, and 0.3.

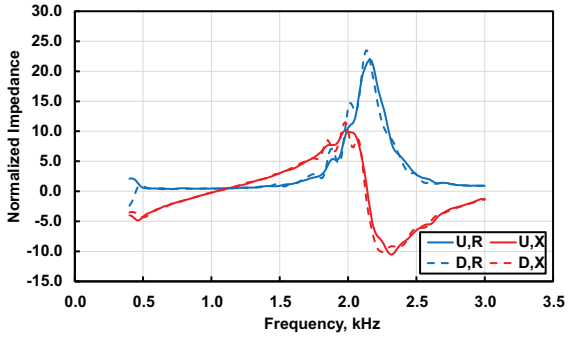

(a) $\mathbf{M_{SP} = 0.0}$.

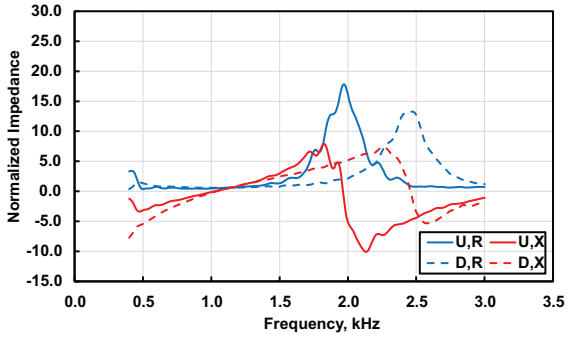

(b) **1D average Mach number,** $M_{SP} = 0.3$.

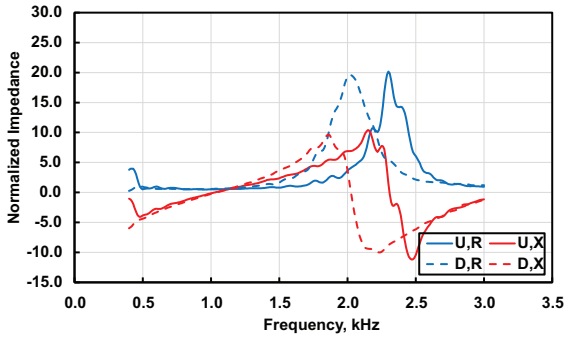

(c) **2D average Mach number,** $M_{SP} = 0.3$.

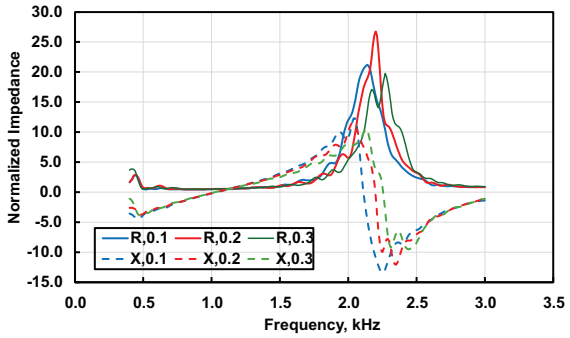

(d) **Upstream source,** $M_{SP} = 0.1, 0.2, 0.3$.

Figure 9: **Educed resistance (R) and reactance (X) spectra for upstream (U) and downstream (D) sources using different versions of the average Mach number; 140 dB source, CSQ3 liner.**

It is the view of the authors that the results presented in Figures 9 and 10 clearly demonstrate that the choice of Mach number to be used in the analysis is critical. Clearly, it is problematic at best to compare impedances educed using average Mach numbers derived from 1D versus 2D measurements. This is particularly true for frequencies near antiresonance.

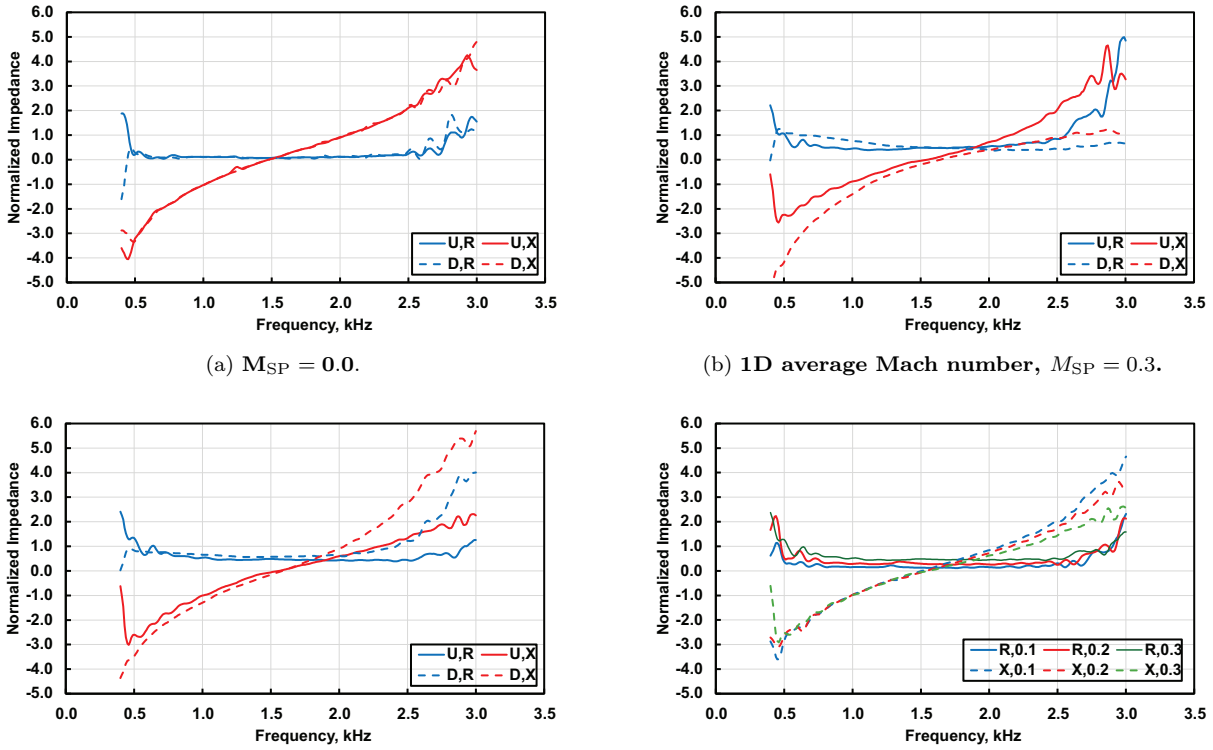

(a) $\mathbf{M_{SP} = 0.0}$.

(b) **1D average Mach number,** $M_{SP} = 0.3$.

(c) **2D average Mach number,** $M_{SP} = 0.3$.

(d) **Upstream source,** $\mathbf{M_{SP} = 0.1, 0.2, 0.3}$.

Figure 10: **Educed resistance (R) and reactance (X) spectra for upstream (U) and downstream (D) sources using different versions of the average Mach number; 140 dB source, IU2 liner.**

Figure 11 provides impedances educed from the CSQ3 data acquired with a source level of 140 dB. All of these impedances are educed using the same exact dataset, with the only difference being the Mach number used in the analysis. Five choices for the average Mach number are considered: 0.231, 0.236, 0.241, 0.246, and 0.251. This covers much of the range between the 1D (0.259) and 2D (0.231) average Mach numbers derived from the flow surveys.

Note that the increment for this demonstration is 0.005. The baseline (zero offset) Mach number (0.241) is chosen because it causes the key features of the impedances educed using the upstream and downstream sources to coalesce. Note that when the analysis Mach number is set to 0.231 (offset of -0.010 from the baseline), the peak resistance with the downstream source is below that for the upstream source. When the analysis Mach number is increased by 0.005 (offset of -0.005), the peak for the downstream source gets closer to that for the upstream source. If the offset is +0.005 (analysis Mach number of 0.246), the peak resistance for the downstream source transitions to be higher than that for the upstream source. Finally, at an offset of +0.010, this shift is even larger. Observe that this very large range of impedances, especially the portion of the results near antiresonance, is achieved with a Mach number range of ±0.01. A similar result is observed for the IU2 liner. Specifically, an analysis Mach number of 0.241 causes the upstream and downstream educed impedance spectra to compare favorably, similar to that observed for the CSQ3 liner.

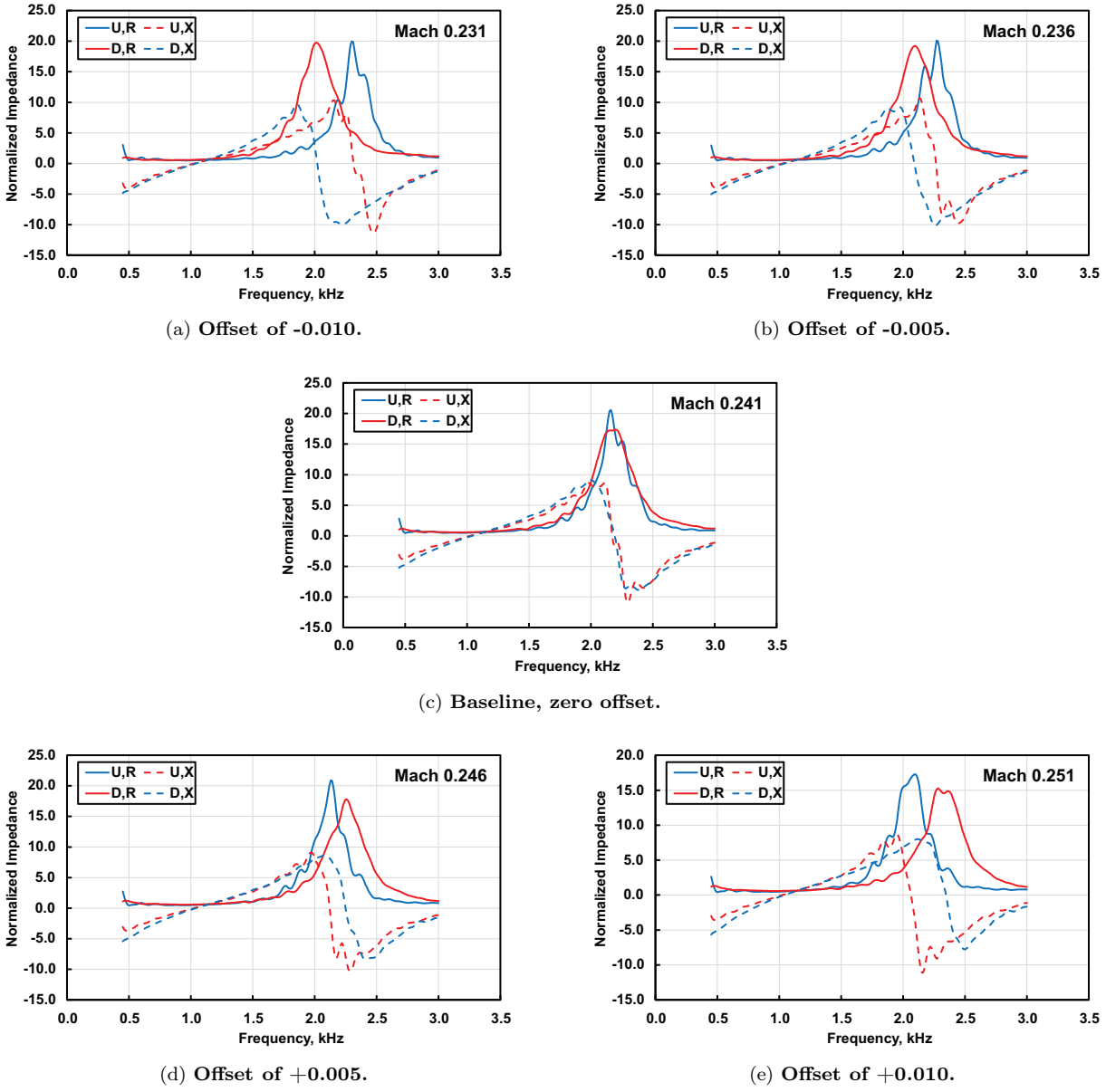

(a) **Offset of -0.010.**

(b) **Offset of -0.005.**

(c) **Baseline, zero offset.**

(d) **Offset of +0.005.**

(e) **Offset of +0.010.**

Figure 11: **Effects of Mach number on educed resistance (R) and reactance (X) spectra for upstream (U) and downstream (D) sources; 140 dB source, CSQ3 liner.**

This is an important point, as it seems obvious that the true average Mach number to be used in the acoustic analysis should be independent of the liner that is installed. It is interesting to note that the preferred analysis Mach number of 0.241 is 0.010 above the 2D average Mach number. Recall that our approach for determining the average Mach number is based on (1) acquiring 2D flow profiles upstream and downstream of the test window, (2) computing average Mach numbers at each axial station, and (3) computing a prorated average of these two Mach numbers based on the distance from those two measurement stations to the axial midpoint of the liner. This process assumes the average Mach number varies linearly over this axial extent. Thus, it is very plausible to accept that the measurement process could be off by 0.01. Regardless, it is critical to use some version of this approach to determine the proper Mach number to be used in the impedance eduction analysis. It is interesting to note that the 2D average Mach number has decreased by about 10% from that measured with a slightly different GFIT configuration in an earlier study.[7] However,

the preferred analysis Mach number based on the assumption that the impedance for a linear liner should be independent of flow direction changed by less than 2%.

V. Concluding Remarks

The NASA Langley Liner Physics Team has acquired a detailed dataset for use in the evaluation of flow direction effects on the acoustic liner impedance eduction process. Measurements are acquired with four acoustic liners designed to cover a range of sensitivities to source sound pressure level and tangential mean flow effects. These measurements include detailed flow profile surveys upstream and downstream of the liner test window, as well as acoustic pressure data over the extent of the test window. These data will soon be supplied to the IFAR partners and will be made available for the general public within the next year. Representative results for two of these liners were presented in the current paper. The first is comprised of a large array of very narrow, long chambers, while the second is an additively manufactured perforate-over-honeycomb liner.

Mean flow surveys were conducted at two axial planes in the NASA Langley Grazing Flow Impedance Tube, upstream and downstream of the test window that typically contains the test liner. These data were used to determine two average Mach numbers in each axial plane. The first was based on a 1D vertical sweep along the spanwise midline of the duct, while the other was a 2D average over the entire plane. A prorated average of the Mach numbers at the two axial planes relative to the axial midpoint of the test liner was used to determine the average Mach number (whether 1D or 2D) to be used in the acoustic analysis. As expected, the 2D average Mach number is always lower than the 1D average Mach number. Impedance spectra educed using each of these average Mach numbers with the Prony method demonstrated the importance of this choice of Mach number.

Based on these results, there are two key features regarding the effects of flow direction on the impedance that is educed for test liners. First, it is imperative to specify a Mach number consistent with the impedance boundary condition used in the impedance eduction process. The results shown in this paper clearly demonstrate that differences as small as 0.01 can result in very significant changes to the educed impedance spectrum, particularly for frequencies near antiresonance. It is suggested that a calibration liner (e.g., the CSQ3 liner used in this study) should be used to experimentally determine the choice of a proper average Mach number to be used in the acoustic analysis. Second, it is important to note that the SPL over the extent of the liner may be dependent on the flow direction. Unfortunately, the test liners chosen for the current study were not sufficiently nonlinear to clearly demonstrate these effects. Regardless, it is well understood that the educed impedance for a nonlinear liner will be affected by changes in the SPL. This difference is not specifically due to the direction of flow, but is instead due to the change in SPL caused by the direction of flow. Regardless, the way in which one describes this phenomenon will likely depend on one's point of view. Besides these two key features, it is certainly possible that there remain additional subtle differences that could be explained by the inclusion of additional physics into the impedance eduction process. However, until the first two effects (average Mach number and SPL) are fully understood, these additional features are considered to be of much less importance.

Acknowledgements

This work was funded by the Advanced Air Transport Technology Project of the NASA Advanced Air Vehicles Program. The authors wish to express thanks to all members of the NASA Langley Liner Physics Team for their efforts in collecting the experimental data.

References

[1]Jones, M. G., Nark, D. M., and Howerton, B. M., "Overview of Liner Activities in Support of the International Forum for Aviation Research," AIAA Paper 2019-2599, May 2019.

[2]Kreitzman, J. R. and Jones, M. G., "Influence of source type on acoustic liner impedance in no flow," Aiaa paper (submitted for publication), June 2024.

[3]Renou, Y. and Auregan, Y., "Failure of the Ingard-Myers Boundary Condition for a Lined Duct: An Experimental Investigation," *Journal of the Acoustical Society of America*, Vol. 130, No. 1, July 2011, pp. 52–60.

[4]Watson, W. R. and Jones, M. G., "Evaluation of Wall Boundary Conditions for Impedance Eduction Using a Dual-Source Method," AIAA Paper 2012-2199, June 2012.

[5]Bodén, H., Zhou, L., Cordioli, J. A., Medeiros, A. A., and Spillere, A. M. N., "On the effect of flow direction on impedance eduction results," AIAA Paper 2016-2727, 2016.

[6]Schulz, A., Weng, C., Bake, F., Enghardt, L., and Ronneberger, D., "Modeling of liner impedance with grazing shear flow using a new momentum transfer boundary condition," AIAA Paper 2017-3377, June 2017.

[7]Nark, D. M., Jones, M. G., and Piot, E., "Assessment of Axial Wavenumber and Mean Flow Uncertainty on Acoustic Liner Impedance Eduction," AIAA Paper 2018-3444, June 2018.

[8]Zhang, P., Huang, Y., Yang, Z., Yang, C., and Jiang, W., "Effect of source direction on liner impedance eduction with consideration of shear flow," *Applied Acoustics*, Vol. 183, No. 108297, 2021.

[9]Bielak, G., Gallman, J., Kunze, R., Murray, P., Premo, J., Kosanchick, M., Hersh, A., Celano, J., Walker, B., Yu, J., Kwan, H. W., Chiou, S., Kelly, J., Betts, J., Follet, J., and Thomas, R., "Advanced Nacelle Acoustic Lining Concepts Development," NASA CR 211672, 2002.

[10]Parrott, T. L. and Jones, M. G., "Parallel-Element Liner Impedances for Improved Absorption of Broadband Sound in Ducts," *Noise Control Engineering Journal*, Vol. 43, No. 6, Nov. 1995.

[11]Howerton, B. M., Vold, H., and Jones, M. G., "Application of Sine Sweep Excitation for Acoustic Impedance Eduction," AIAA Paper 2019-2487, May 2019.

[12]Watson, W. R., Carpenter, M. H., and Jones, M. G., "Performance of Kumaresan and Tufts Algorithm in Liner Impedance Eduction with Flow," *AIAA Journal*, Vol. 53, No. 4, April 2015, pp. 1091–1102.

[13]de Prony, R., "Essai Éxperimental et Analytique: Sur Les Lois de la Dilatabilité de Fluides Élastique et sur Celles de la Force Expansive de la Vapeur de L'alkool, Àdifférentes Temperatures," *Journal de l'école Polytechnique*, Vol. 1, No. 22, 1795, pp. 24–76.

[14]Jones, M. G., Watson, W. R., and June, J. C., "Optimization of Microphone Locations for Acoustic Liner Impedance Eduction," AIAA Paper 2015-3271, June 2015.

[15]Myers, M. K., "On the Acoustic Boundary Condition in the Presence of Flow," *Journal of Sound and Vibration*, Vol. 71, No. 3, 1980, pp. 429–434.

[16]Eversman, W. and Gallman, J. M., "Impedance Eduction with an Extended Search Procedure," *AIAA Journal*, Vol. 49, No. 9, September 2011, pp. 1960–1970.